Published OnlineFirst August 31, 2010; DOI: 10.1158/1535-7163.MCT-10-0486

Molecular Therapy Targeting Sonic Hedgehog and Hepatocyte Growth Factor Signaling in a Mouse Model of Medulloblastoma

Valerie Coon[1], Tamara Laukert[1], Carolyn A. Pedone[1], John Laterra[2], K. Jin Kim[3], and Daniel W. Fults[1]

Abstract

The use of genetically engineered mice has provided insights into the molecular pathogenesis of the pediatric brain tumor medulloblastoma and revealed promising therapeutic targets. Ectopic expression of Sonic hedgehog (Shh) in cerebellar neural progenitor cells induces medulloblastomas in mice, and coexpression of hepatocyte growth factor (HGF) enhances Shh-induced tumor formation. To determine whether Shh + HGF–driven medulloblastomas were responsive to Shh signaling blockade and whether treatment response could be enhanced by combination therapy targeting both HGF and Shh signaling pathways, we carried out a survival study in mice. We induced medulloblastomas by retrovirus-mediated expression of Shh and HGF, after which we treated the mice systemically with (*a*) HGF-neutralizing monoclonal antibody L2G7, (*b*) Shh signaling inhibitor cyclopamine, (*c*) Shh-neutralizing monoclonal antibody 5E1, (*d*) L2G7 + cyclopamine, or (*e*) L2G7 + 5E1. We report that monotherapy targeting either HGF signaling or Shh signaling prolonged survival and that anti-HGF therapy had a more durable response than Shh-targeted therapy. The effect of L2G7 + 5E1 combination therapy on cumulative survival was equivalent to that of L2G7 monotherapy and that of L2G7 + cyclopamine therapy was worse. The principal mechanism by which Shh- and HGF-targeted therapies inhibited tumor growth was a potent apoptotic death response in tumor cells, supplemented by a weaker suppressive effect on proliferation. Our observation that combination therapy either failed to improve or even reduced survival in mice bearing Shh + HGF–induced medulloblastomas compared with monotherapy underscores the importance of preclinical testing of molecular-targeted therapies in animal models of tumors in which the targeted pathways are known to be active. *Mol Cancer Ther; 9(9); 2627–36. ©2010 AACR.*

Introduction

Advances in cancer treatment will require preclinical testing in animal models that accurately recapitulate the molecular pathogenesis of human disease. Although cell culture methods are commonly used as initial screens of anticancer drugs, subsequent clinical trials have shown that these methods often produce false-positive results (reviewed in ref. 1). *In vitro* drug testing is limited by the fact that tumor cells, when propagated in culture, acquire mutations that are not tumor-initiating events *in vivo*. Moreover, cell culture systems fail to model the complex tumor-host interactions that characterize spontaneously arising tumors. Tumor xenograft models, in which established cancer cell lines are implanted in mice, maintain tumor-host interactions but are limited by the lack of stepwise genetic changes that occur naturally during tumor progression. Genetically engineered mice are more realistic and stringent platforms for preclinical testing of anticancer agents than cell culture and xenograft models. Not only are the initiating genetic events defined, but tumor progression also takes place in a native environment in which tumor-host interactions are preserved.

Medulloblastomas are malignant brain tumors that arise in the cerebellum in children. Pediatric oncologists currently stratify patients into average-risk and high-risk categories according to three prognostic factors: age, extent of surgical resection, and metastatic disease (reviewed in ref. 2). Short survival times are associated with younger patient age (<4 years), incomplete surgical resection, or dissemination of tumor cells to cerebrospinal fluid spaces or extraneural sites. Aggressive treatment regimens that combine maximum surgical resection, craniospinal radiation, and multiple drug chemotherapy result in 5-year survival rates of >70% for

Authors' Affiliations: [1]Department of Neurosurgery, University of Utah School of Medicine, Salt Lake City, Utah; [2]Department of Neurology, The Kennedy Krieger Institute and Johns Hopkins School of Medicine, Baltimore, Maryland; and [3]Galaxy Biotech, LLC, Mountain View, California

Note: V. Coon and T. Laukert contributed equally to this work.

Corresponding Author: Daniel W. Fults, Department of Neurosurgery, University of Utah School of Medicine, 175 North Medical Drive East, Salt Lake City, UT 84132. Phone: 801-581-6908; Fax: 801-581-4385. E-mail: daniel.fults@hsc.utah.edu

doi: 10.1158/1535-7163.MCT-10-0486

Published OnlineFirst August 31, 2010; DOI: 10.1158/1535-7163.MCT-10-0486

newly diagnosed, average-risk patients (3). Despite these encouraging statistics, treatment-related neurotoxicity causes growth retardation, endocrine dysfunction, and progressive cognitive impairment in long-term survivors (4, 5). Thus, there is a critical need to identify molecules that can be targeted therapeutically to circumvent the toxic side effects of treatment.

The use of genetically engineered mice has provided insights into the molecular pathogenesis of medulloblastoma and exposed promising therapeutic targets. Several different methods of activating the Sonic hedgehog (Shh) signaling pathway in the developing cerebellum can induce tumors in mice that closely resemble human medulloblastomas. These methods include (*a*) targeted deletion of the *Patched* gene, which encodes the inhibitory receptor for Shh (6), (*b*) ectopic expression of Shh by retroviral transfer (7, 8), and (*c*) transgenic overexpression of Smoothened, a positive effector of Shh signaling (9, 10). Cell type–specific activation of Shh signaling has shown that medulloblastomas could originate from either multipotent neural stem cells (11) or granule neuron precursor cells (12).

A large body of evidence from studies of mice and humans indicates that activation of cell signaling by hepatocyte growth factor (HGF) promotes tumor growth. HGF, also known as scatter factor, is a multifunctional growth factor that drives cell cycle progression, blocks apoptosis, stimulates cell motility, and promotes angiogenesis (reviewed in refs. 13 and 14). These diverse effects of HGF are all mediated by its cell surface receptor, the transmembrane tyrosine kinase encoded by the proto-oncogene *c-Met* (15). The fact that HGF strongly inhibits apoptosis, partly by activating Akt via the phosphatidylinositol 3-kinase and Src signal transduction pathways, makes HGF an attractive target for cancer therapy (16, 17). In principle, interrupting the strong antiapoptotic effect of HGF, to which cancer cells can become addicted, could induce oncogenic shock and consequently trigger the rapid death of tumor cells (18).

Both *HGF* and *c-Met* are frequently expressed in human medulloblastomas, and the elevated mRNA levels of these genes predict an unfavorable prognosis for patients (19). The fact that kinase-activating mutations in the *c-Met* gene have not been reported in medulloblastomas indicates that HGF:c-Met signaling in these tumors is driven by a ligand-dependent, autostimulatory loop, which could be interrupted via the high specificity and avidity of monoclonal antibodies (mAbs). In support of this mechanism, we reported previously that overexpression of HGF enhances Shh-induced medulloblastoma formation in mice and that systemic administration of an HGF-neutralizing mAb (L2G7) prolongs survival in mice bearing Shh + HGF–induced medulloblastomas (20). We also observed that cumulative survival of mice treated with the anti-HGF mAb continued to decline throughout the treatment period.

Sustained tumor growth in the face of HGF blockade might be explained by unchecked Shh stimulation. Consistent with this possibility, pharmacologic inhibition of Hedgehog signaling by antagonists of Smoothened promotes the regression of medulloblastomas in $Patched^{+/-}/p53^{-/-}$ mice (21, 22). Medulloblastomas arise spontaneously in $Patched^{+/-}$ mice in response to hyperactive Hedgehog signaling (23). Germ line deletion of the *p53* tumor suppressor gene in $Patched^{+/-}$ mice increases the incidence and decreases the latency of tumor formation, an effect that has been exploited to increase the power of preclinical testing studies (24).

We asked whether Shh + HGF–driven medulloblastomas were responsive to Shh signaling blockade and whether treatment response could be enhanced by combination therapy targeting both HGF and Shh. To answer these questions, we carried out a survival study in mice, in which we first induced medulloblastomas by retrovirus-mediated expression of Shh and HGF. We then treated the mice systemically, alone or in concert, with agents that inhibit HGF and Shh signaling: (*a*) HGF-neutralizing mAb L2G7, (*b*) Shh signaling inhibitor cyclopamine, (*c*) Shh-neutralizing mAb 5E1, (*d*) L2G7 + cyclopamine, or (*e*) L2G7 + 5E1.

Materials and Methods

In vivo somatic cell gene transfer in transgenic mice

To test the therapeutic efficacy of molecules that block HGF and Hedgehog signaling, we used a version of the RCAS/*tv-a* somatic cell gene transfer system that enabled us to induce medulloblastomas in mice by overexpressing HGF and Shh in $Nestin^{+}$ neural progenitor cells in the cerebellum. This system uses a replication-competent, avian leukosis virus, splice acceptor (RCAS) vector, derived from the subgroup A avian leukosis virus (ALV-A), and a transgenic mouse line (*Ntv-a*) that produces TVA (the cell surface receptor for ALV-A) under control of the *Nestin* gene promoter (25). Nestin is an intermediate filament protein that is expressed by neural stem cells prior to their commitment to neuronal or glial differentiation. When mammalian cells are transduced with RCAS vectors, viral replication does not occur. Instead, the RCAS provirus integrates into the host cell genome, and the transferred gene is expressed as a spliced message under the control of the constitutive retroviral promoter (long-terminal repeat sequence).

To transfer genes via RCAS vectors, we injected retrovirus packaging cells (DF-1 cells transfected with and producing recombinant RCAS retrovirus) into the lateral cerebellum from an entry point just posterior to the lambdoid suture of the skull (bilateral injections of 10^5 cells in 1 to 2 μL of PBS). The cell pellets were prepared by mixing equal numbers of both retrovirus-producing cells (Shh + HGF). We injected mice within 72 hours after birth because the number of Nestin-expressing neural progenitor cells, which produce ALV-A receptors in *Ntv-a* mice, decreases progressively afterward. The mice were sacrificed as soon as they showed signs of increased intracranial pressure, indicated by enlarging head circumference

Published OnlineFirst August 31, 2010; DOI: 10.1158/1535-7163.MCT-10-0486

(a sign of hydrocephalus), gait ataxia, or failure to thrive. Asymptomatic mice were sacrificed at the chosen experimental end points. The brains were fixed in formalin, divided into quarters by parallel incisions in the coronal plane, embedded in paraffin, and sectioned for immunocytochemical analysis.

Transgenic mice

The use of mice in this study was approved by the Institutional Animal Care and Use Committee of the University of Utah. Production of the *Ntv-a* mouse line, in which expression of the *tv-a* transgene is driven by promoter/enhancer sequences of the *Nestin* gene, has been described previously (25). Because of the breeding strategy used to introduce the transgene, *Ntv-a* mice are hybrids composed of the following genetic strains: C57BL/6, BALB/C, FVB/N, and CD1.

Retroviral vector construction

Construction of the RCAS-HGF and RCAS-Shh vectors was described previously (8, 20). Briefly, the vectors were prepared by ligating a PCR-generated cDNA corresponding to the complete coding sequence of the human *HGF* gene or the chicken *Shh* gene into the parent retroviral vector RCASBP(A) (ref. 26). To produce live virus, we transfected plasmid versions of RCAS vectors into immortalized chicken fibroblasts (DF-1 cells) and allowed them to replicate in culture.

Therapeutic agents

Cyclopamine was purchased from LC Laboratories. A 10 mg/mL stock solution was prepared by dissolving cyclopamine in sodium phosphate/citrate buffer (pH 3.0) containing 10% (w/v) 2-hydroxypropyl-β-cyclodextrin (Sigma-Aldrich), then aliquoted and stored at −20°C. Before it was injected into the mice, this stock solution was diluted 10-fold in PBS, and the pH was adjusted to 7.0 using 1 mol/L of NaOH. The generation and characterization of mouse mAbs 5E1 (anti-Shh) and L2G7 (anti-HGF) and nonspecific, isotype-matched, control antibody 5G8 have been described previously (27, 28).

Immunocytochemistry and microscopy

To analyze protein expression in tissue sections, we used immunoperoxidase staining methods that we have described previously (8). Briefly, tissue sections (4 μm) were deparaffinized, rehydrated, autoclaved in a citrate-based antigen retrieval solution (Vector Laboratories) for 5 minutes, and then cooled to room temperature before application of primary antibody. Immunoreactive staining was visualized using an avidin-biotin complex technique with diaminobenzidine as the chromogenic substrate and toluidine blue as a nuclear counterstain. Tissue sections were visualized using a Zeiss Axiovert 200 microscope and photomicrographs were captured using an AxioCam high-resolution CCD camera and Axiovision imaging software (Carl Zeiss International).

Quantitative analysis of apoptosis, proliferation, and signaling responses

To measure apoptosis, proliferation, and HGF and Shh signaling pathway responses, we used the following quantitative immunostaining method, which generates an index that represents the percentage of positively stained cells in each tumor. This index was handled as a continuous variable in statistical computations. Apoptosis was quantified by immunostaining formalin-fixed, paraffin-embedded tissue sections with an antibody against cleaved caspase-3 (Asp175; Cell Signaling Technology). To calculate the apoptotic index, we used Adobe Photoshop CS4 software to count the number of pixels corresponding to stained and unstained cells in digitized photomicrographs of 10 microscope fields (viewed through a ×40 objective) and then we averaged the percentage of positive pixels from 8 to 11 different tumors in each treatment group. The microscopic fields were randomly selected in tumors that contained more than 10 fields (×40 objective), and the fields were contiguous and nonoverlapping in smaller tumors. Because of the high cell density in medulloblastomas, this method counts $>2 \times 10^3$ cells in each tumor specimen. Cell counts were done by two independent observers. Proliferation index was determined by the same method using a polyclonal antibody against Ki67, a nuclear protein expressed during cell cycle phases G_1-M (Vector Laboratories). To assess Hedgehog signaling activity, we used rabbit polyclonal antibody 26056 (Abcam), which detects nuclear transcription factor Gli2. To assess HGF:c-Met signaling, we used rabbit mAb D26 (Cell Signaling Technology), which detects phosphotyrosine residues Y1232/1233 (mouse) on the activated c-Met receptor tyrosine kinase.

Results

Efficacy of HGF- and Shh-targeted monotherapy in a mouse model of medulloblastoma

We used the RCAS/*tv-a* gene transfer system as a testing platform because we can induce medulloblastomas with high efficiency (78% tumor incidence within 3 months) when we inject RCAS vectors carrying Shh and HGF into the cerebella of newborn *Ntv-a* mice (20). The tumors arise in the dorsolateral cerebellum at the injection sites and cause obstructive hydrocephalus (Fig. 1A and B). Microscopically, most of the tumors resemble the classic subtype of human medulloblastomas, which is characterized by homogenous sheets of densely packed, rapidly dividing cells containing hyperchromatic nuclei and scant cytoplasm (Fig. 1C). Approximately 10% of tumors induced by Shh + HGF resemble a less common subtype called medulloblastoma with extensive nodularity (MBEN; ref. 29). These MBEN-like tumors contained clusters and rows of neurocytic cells that have round nuclei (Fig. 1D). Positive immunostaining for neuronal differentiation markers βIII-tubulin, NeuN, and synaptophysin was localized to the neurocytic cells in the MBEN-like tumors and was homogeneously distributed in the

Published OnlineFirst August 31, 2010; DOI: 10.1158/1535-7163.MCT-10-0486

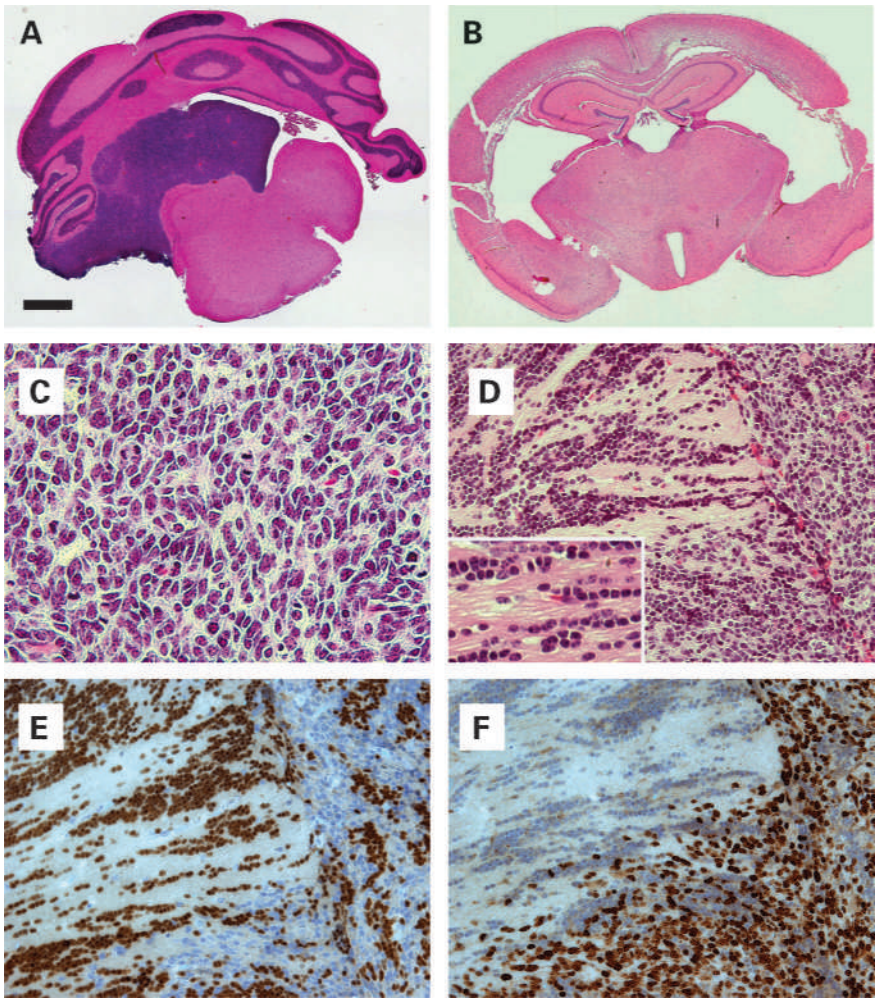

Figure 1. Histopathology of medulloblastomas induced by Shh + HGF. A and B, coronal brain sections showing tumor in the cerebellum and fourth ventricle (A) and obstructive hydrocephalus in the forebrain (B; H&E). C, classic medulloblastoma pattern showing homogeneous sheets of undifferentiated tumor cells (H&E). D, MBEN pattern in which round, neurocytic-appearing tumor cells are arrayed in a linear pattern (top left and inset) adjacent to an area of disorganized cytoarchitecture characteristic of the classic pattern (right; H&E). E, immunoperoxidase staining showing that MBEN areas (left) have abundant immunoreactivity for neuronal differentiation marker NeuN compared with classic-appearing areas (right). F, immunoperoxidase staining showing that Ki67 staining is absent in the MBEN area (left) compared with the actively proliferating cells in the classic-appearing area (right). Scale bars, 500 μm (A and B), 25 μm (C and D, inset), and 50 μm (D–F).

classic-appearing tumors (Fig. 1E shows results with NeuN). The neurocytic cells show little proliferation as measured by Ki67 immunostaining (Fig. 1F).

We injected newborn *Ntv-a* mice with RCAS-Shh and RCAS-HGF to induce medulloblastomas. Two weeks later, we initiated treatment with agents that inhibit Shh and HGF signaling, according to the protocol shown in Table 1. To inhibit HGF signaling, we used mAb L2G7, which has been shown to neutralize the ability of HGF to stimulate proliferation, scattering, and survival of cells in culture (28). Systemic administration of L2G7 prolongs the survival of mice bearing intracerebral xenografts of human HGF^+/c-Met^+ glioblastomas (28) as well as *Ntv-a* mice bearing Shh + HGF–induced medulloblastomas (20).

To block Hedgehog signaling, we took two different approaches. One approach was to use the alkaloid cyclopamine, derived from the corn lily *Veratrum californicum*. Cyclopamine binds and inhibits Smoothened, which is the positively responding component of the Shh/Patched receptor apparatus (30). Work in other laboratories has shown that systemic administration of cyclopamine or a more potent, benzimidazole derivative of cyclopamine, promotes tumor regression, and prolongs survival in $Patched^{+/-}/p53^{-/-}$ mice (21, 22). The dosing regimen we used generates micromolar concentrations of cyclopamine in the serum of adult mice (31) and, when administered to pregnant mice, reduces *Gli1* mRNA levels in fetal neocortex (32). Our second approach was to use Shh-neutralizing mAb 5E1 (27), which has been shown to block proliferation of granule neuron precursor cells during normal cerebellar development *in vivo* (33).

We started treatment 2 weeks after RCAS injection because that was the earliest time point at which we had observed tumors in our previous studies (20). The primary experimental end point was survival time during a 4-month observation period. Animals were monitored daily for signs of neurologic impairment, at the onset of which they were sacrificed and analyzed immediately. All remaining mice were sacrificed 4 months after the

Published OnlineFirst August 31, 2010; DOI: 10.1158/1535-7163.MCT-10-0486

initial RCAS injection. We chose a 4-month observation period for the survival study to allow the comparison of our current and previous results. The number of experimental animals (60 per treatment group) was calculated based on the 78% incidence of Shh + HGF–induced tumor formation that we observed during a 3-month observation period and the assumption that treatment with L2G7, cyclopamine, and 5E1 would neutralize the effect of the targeted signaling pathways completely. The limited availability of 5E1 antibody required us to enroll only 34 mice in the 5E1 treatment group. A control group of mice was injected with nonspecific antibody 5G8.

We used Kaplan-Meier analysis to compare survival times among the five groups (Table 1; Fig. 2A). Three mice (two in the L2G7 group and one in the combination therapy group) died from injection-related brain hemorrhage before starting treatment and were therefore excluded from further analysis. Median survival time was 111 days in the L2G7 group compared with 23 days in the 5G8 control group ($P = 0.03$ by log-rank test). We observed a similarly strong survival advantage with L2G7 treatment in a previous, independent study (20). The median survival times of mice treated with cyclopamine (62 days) and 5E1 (102 days) were significantly longer than that of control mice treated with 5G8 ($P = 0.04$). The response to Hedgehog pathway–targeted therapy was less durable than the response to HGF-targeted therapy. The curves depicted in Fig. 2A show that the cumulative survival of cyclopamine-treated mice decreased to below that of L2G7-treated mice 46 days after starting treatment. The 5E1 and L2G7 survival curves intersected after 81 days of treatment.

Variable responses to Shh + HGF–targeted combination therapy

Surprisingly, the median survival of mice treated with L2G7 + cyclopamine in combination (47 days) was less than that of mice treated with L2G7 (111 days) or cyclopamine (62 days) alone (Fig. 2A; Table 1). Drug toxicity was an unlikely cause for the loss of individual effectiveness when L2G7 and cyclopamine were used in combination. We observed no effects in the mice suggestive of drug toxicity, such as changes in body weight or grooming behavior. Moreover, the fact that the incidence of histologically verified tumors in the L2G7 + cyclopamine group (63%) was comparable with that in the L2G7 (48%) and cyclopamine (75%) groups indicated that the death of mice in all groups was caused by brain tumor growth, not drug toxicity.

Our observation that 5E1 monotherapy conferred a stronger survival advantage than cyclopamine monotherapy suggested to us that response to combination therapy might be improved by blocking Hedgehog signaling using mAb 5E1, instead of cyclopamine. To address this possibility, we undertook a second study in which we compared survival times in mice bearing Shh + HGF–induced medulloblastomas when treated with L2G7 versus L2G7 + 5E1. We used the same protocol described above except that the observation time was reduced to 90 days, the time during which we observed a survival difference between 5E1 and L2G7 treatment groups in the first study. We analyzed 68 mice in the L2G7 group and 71 in the L2G7 + 5E1 group. Cumulative survival of mice treated with L2G7 + 5E1 in combination was equivalent to that of mice treated with L2G7 alone ($P = 0.4$ by log-rank test; Fig. 2B).

Mechanisms of antitumor activity

We carried out a detailed histochemical analysis of the brains from mice in the six treatment groups from the two survival studies described above. The brains were fixed, sectioned, and stained with H&E. Specimens were scored as positive if they contained tumors large enough to show a clear cytologic pattern of medulloblastoma. Among mice that were scored as uncensored events, the incidence of histologically verified tumors was high (68–86%), indicating that cumulative survival in our mouse model system accurately measures the effect of each therapeutic agent on cancer-related death.

To assess the effect of treatment on tumor cell proliferation and apoptosis, we quantified immunoreactive staining for Ki67 and cleaved caspase-3 in tumors from 8 to 11 different mice from each treatment group. We analyzed all mice scored as uncensored events, in which tumors were large enough to count cells in at least 10 microscopic

Table 1. Four-month survival analysis of *Ntv-a* mice with Shh + HGF–induced medulloblastomas

Therapeutic agent	Dosing regimen	No. of mice analyzed	Median survival (d)	*P*
5G8	2.5 mg/kg i.p. twice weekly	60	23	—
L2G7	2.5 mg/kg i.p. twice weekly	58	111	0.03
Cyclopamine + 5G8	10 mg/kg i.p. every other day + 5G8	60	62	0.04
L2G7 + cyclopamine	See above regimens	59	47	0.8
5E1	5.0 mg/kg i.p. twice weekly	34	>102	0.04

NOTE: *P* values were derived from log-rank tests comparing cumulative survival of each test group with 5G8 control. The *P* value for the cyclopamine group was calculated over a 90-d observation period.

Published OnlineFirst August 31, 2010; DOI: 10.1158/1535-7163.MCT-10-0486

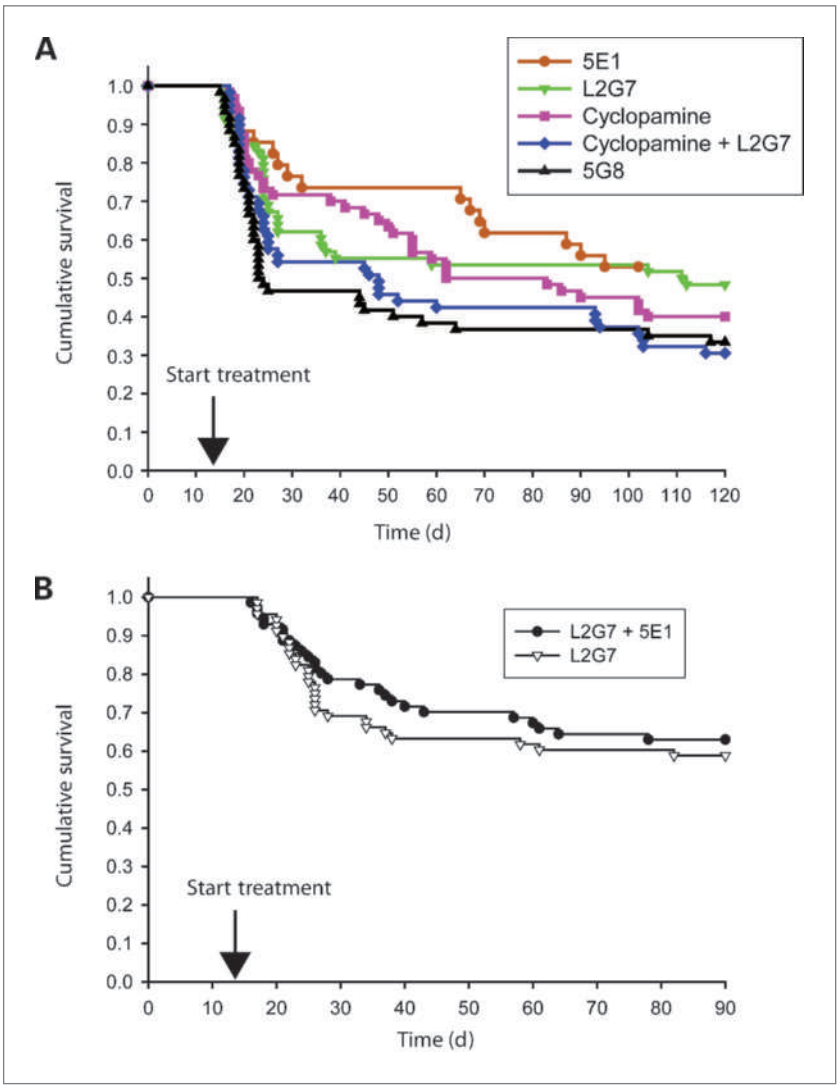

Figure 2. Response to Shh- and HGF-targeted therapy in mice with medulloblastomas. Kaplan-Meier survival analysis of mice injected with RCAS-Shh and RCAS-HGF on day 0 and then treated with the indicated therapeutic agents starting on day 14 (arrow). A and B, results from two independent experiments.

fields (×40 objective). The median ages of mice from which tumors were sampled were comparable among the treatment groups. We assessed the statistical significance of intergroup differences in apoptotic index and proliferation index (percentage of positive cells) using ANOVA and Fisher's protected least significant difference test. The positive effects on overall survival among the six different treatment regimens correlated with decreased proliferation (Fig. 3A) and increased apoptosis in tumor cells (Fig. 3B). The mean proliferation indices of tumors from the L2G7 group (50%) and cyclopamine group (52%) were less than that of the 5G8 control group (65%; $P = 0.003$ and 0.01, respectively). By contrast, the proliferation index in the L2G7 + cyclopamine group (61%) and the L2G7 + 5E1 group (60%) did not differ significantly from that of controls.

Intergroup differences were greater for apoptosis stimulation than for proliferation suppression. For example, the addition of cyclopamine to 5G8 increased the apoptotic index of treated tumors from 0.8% to 2.1%, a 2.6-fold increase ($P = 0.0002$). The same treatment reduced the proliferation index from 65% to 52%, a 0.8-fold decrease ($P = 0.01$). Compared with 5G8, L2G7 treatment increased apoptosis by 2.3-fold ($P = 0.0001$) while reducing proliferation by only 1.3-fold ($P = 0.01$). This more potent effect of therapy on apoptosis induction compared with proliferation suppression might be explained by the very high percentage of cells advancing through the cell cycle (>70% proliferation index) in response to forced expression of Shh and HGF. Paradoxically, adding Hedgehog inhibitors to L2G7 generated less apoptosis than treating animals with Hedgehog inhibitors and L2G7 alone (Fig. 3B). Taken together, the above-described results indicate that the principal mechanism by which Shh- and HGF-targeted therapies inhibited medulloblastoma growth *in vivo* was a potent apoptotic death response in tumor cells, supplemented by a weaker suppressive effect on cell cycle progression.

Published OnlineFirst August 31, 2010; DOI: 10.1158/1535-7163.MCT-10-0486

To analyze the activity of the targeted signaling pathways, we did quantitative immunostaining of brain tissue sections using antibodies that detect signaling proteins downstream of Shh and HGF. To assess Shh signaling activity, we probed tissue sections with an antibody against Gli2, a transcription factor that accumulates in the nucleus in response to Shh stimulation (34). Monotherapy with cyclopamine and 5E1 lowered the percentage of tumor cells showing nuclear Gli2 staining (Gli2 index) compared with 5G8 or L2G7 treatment (Fig. 4A). The addition of cyclopamine or 5E1 to L2G7 also suppressed Gli2 expression even though these combination therapies did not enhance survival compared with L2G7 monotherapy.

To assess HGF signaling, we used an antibody that detects phosphotyrosine residues on c-Met (Y1232/1233 in mouse), which are critical for c-Met tyrosine kinase activation consequent to HGF binding (13). As expected, L2G7 monotherapy suppressed c-Met phosphorylation compared with 5G8 control, and cyclopamine or 5E1 monotherapy did not change the c-Met phosphorylation state (Fig. 4B). The addition of cyclopamine or 5E1 to L2G7 increased the percentage of pc-Met$^+$ tumor cells almost to the level that was observed in 5G8-treated tumors, indicating that Shh pathway suppression reversed the inhibition of HGF:c-Met signaling, at least partially.

Discussion

The challenge in molecular-targeted therapeutics is to identify those signal transduction pathways on which cancer cells have become dependent for their growth and survival. By interrupting these pathways, oncologists hope to arrest tumor cell growth or induce apoptosis more effectively than can be accomplished using cytotoxic chemotherapy and radiation, which impede the growth of cancer cells via nonspecific DNA damage. An emerging theme in cancer therapeutics is that compounds that block specific signaling pathways will be maximally effective against tumors in which the targeted pathway is pathologically hyperactive. For that reason, it is important to test new therapeutic agents in experimental systems that allow the investigator to control which oncogenic signaling pathways are activated.

Models of human medulloblastoma using genetically engineered mice have shown that aberrant activation of the developmentally important Hedgehog signaling pathway in cerebellar neuron precursor cells could initiate medulloblastoma formation. The fact that pharmacologic inhibition of Hedgehog signaling prolongs the survival of *Patched*$^{+/-}$/*p53*$^{-/-}$ mice, in which medulloblastomas arise spontaneously, and our *Ntv-a* mice, in which tumors are induced by forced expression of Shh,

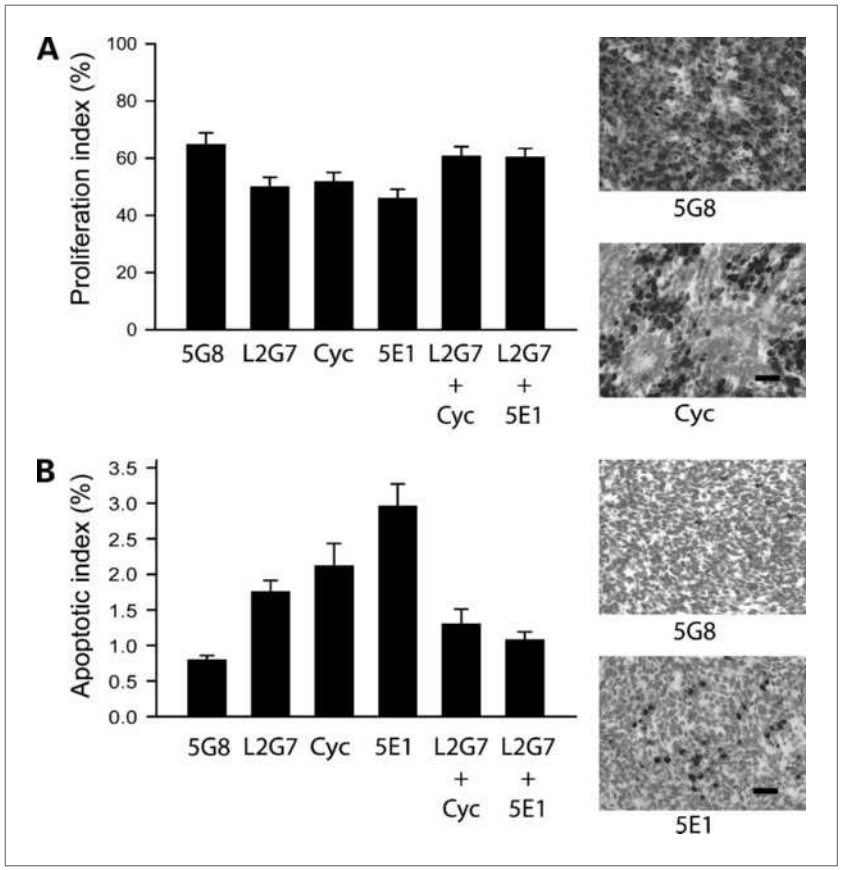

Figure 3. Analysis of proliferation and apoptosis in Shh + HGF–induced medulloblastomas. Bar graphs and representative photomicrographs showing the percentage (mean ± SEM) of tumor cells with positive immunoreactive staining for Ki67 (proliferation index; A) and cleaved caspase-3 (apoptotic index; B) in Shh + HGF–induced medulloblastomas from mice treated with the indicated therapeutic agents. Scale bars, 25 μm.

Published OnlineFirst August 31, 2010; DOI: 10.1158/1535-7163.MCT-10-0486

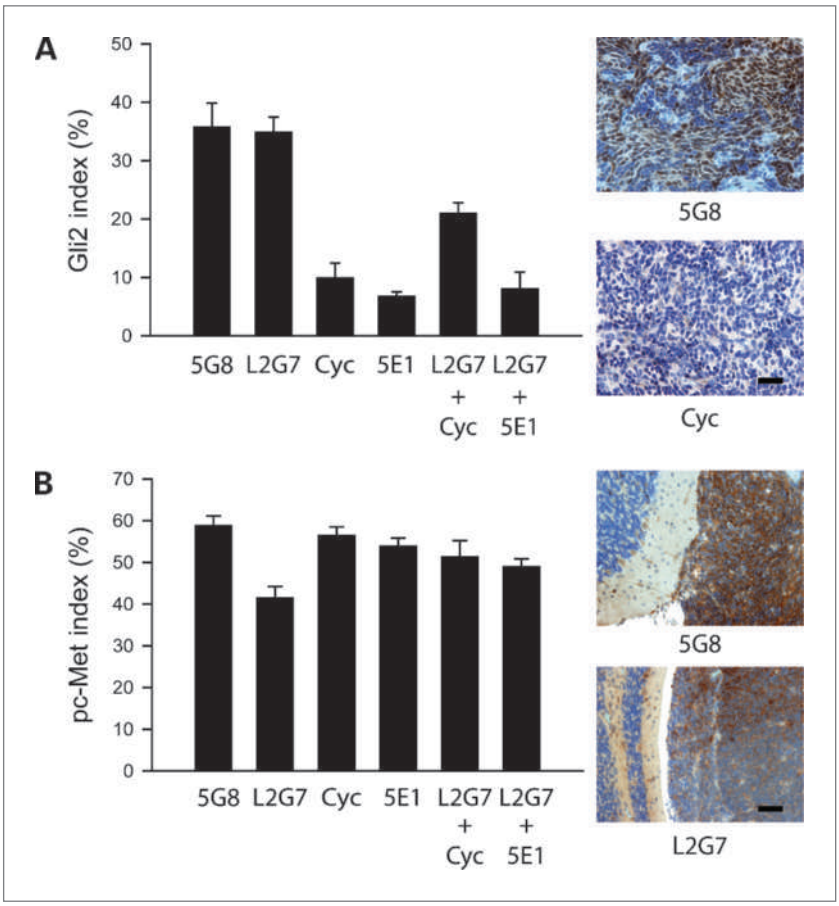

Figure 4. Analysis of Shh and HGF signaling in response to molecular-targeted therapy. Bar graphs and representative photomicrographs showing the percentage (mean ± SEM) of tumor cells with positive immunoreactive staining for Gli2 in the nucleus (Gli2 index; A) and phosphorylated c-Met in the cytoplasm (pc-Met index; B) in medulloblastomas from mice treated with the indicated therapeutic agents. Phototmicrographs in B show pc-Met$^+$ tumor cells (right) adjacent to cerebellar cortex (left). Scale bars, 25 μm (A) and 50 μm (B).

indicates that sustained Hedgehog signaling also plays a role in tumor maintenance. The hope that Hedgehog-targeted therapy might be effective for medulloblastoma patients was stimulated recently by a report of an adult with widely metastatic medulloblastoma, who was treated with Smoothened inhibitor GDC-0449 (35). The patient showed a rapid treatment response, as shown by the regression of metastatic tumors and a reduction of the patient's pain. Treatment response was only temporary because of the emergence of cells expressing a *Smoothened* point mutation rendering GDC-0449 inactive (36). The progressive decline in cumulative survival of cyclopamine-treated mice in our study (Fig. 1A) might be caused by a similar mechanism of drug resistance.

The efficacy of HGF-targeted therapy against medulloblastoma has not been tested in humans. A phase I clinical trial is currently under way to test the safety of a humanized version of L2G7 (TAK-701) in adult patients with nonhematologic malignancies. A phase II clinical trial is now testing the efficacy of HGF-neutralizing mAb AMG102 as a single, systemically delivered agent in patients with glioblastoma multiforme, a malignant glial tumor in which HGF:c-Met signaling is hyperactive (37). The rationale for this trial came from the results of two preclinical studies showing the regression of human HGF$^+$/c-Met$^+$ glioblastoma xenografts in mice that were treated with HGF-neutralizing mAbs (28, 38). Our results, which were obtained from HGF-expressing tumors, indicate that HGF-targeted therapy will likely be effective for patients in whom medulloblastoma growth is driven by an HGF:c-Met autostimulatory feedback loop.

An emerging concept in pediatric oncology is that medulloblastomas comprise a diverse group of tumors in which subtypes arise by transformation of different populations of neural stem cells in response to the activation of different molecular signaling pathways (39–41). This concept predicts that treatment regimens for medulloblastoma patients will be maximally effective if they target those signaling pathways that are activated in specific medulloblastoma subtypes. We cannot conclude that the results of this preclinical testing study are relevant to all medulloblastomas, but rather to those subtypes that are dependent on Shh and HGF signaling.

Work in other laboratories has shown that Hedgehog-targeted therapy inhibits the growth of medulloblastomas in mice principally by suppressing tumor cell proliferation (21, 22). Our observation that cyclopamine and 5E1 affected apoptosis more potently than proliferation might be explained by the fact that the previous studies were carried out using *Patched*$^{+/-}$/*p53*$^{-/-}$ mice, in which

Published OnlineFirst August 31, 2010; DOI: 10.1158/1535-7163.MCT-10-0486

p53-mediated apoptosis is disabled. Loss-of-function mutations in the *p53* gene, which occur in 16% of human medulloblastomas, are associated with a high rate of recurrence and short survival time (42). Thus, treatment responses in our *p53* wild-type mice might not accurately predict response in this aggressive, *p53* mutant subtype.

A large body of experimental evidence now supports the notion that cancer growth is driven by simultaneous firing of multiple signaling pathways in individual tumor cells. Accordingly, the response of cancer patients to treatment will be enhanced by combining drugs to target multiple signaling pathways. The complex interaction among signal transduction pathways, however, makes it impossible to predict *in vivo* responses to combination therapies. For example, a randomized clinical trial was carried out in 755 patients with metastatic colorectal cancer to determine whether treatment response could be improved by adding the epidermal growth factor receptor–neutralizing mAb cetuximab to a proven regimen consisting of fluoropyrimidine-based chemotherapy and antivascular endothelial growth factor mAb bevacizumab (43). Both of the mAbs had previously shown efficacy when used as single agents or in combination with cytotoxic chemotherapy. Surprisingly, the addition of cetuximab to bevacizumab plus chemotherapy shortened progression-free survival times and lowered quality-of-life scores.

Our results reported here in a defined, Shh + HGF–induced medulloblastoma model mirror these clinical results because Shh pathway inhibitors that were effective as monotherapies either failed to enhance or actually abrogated the antitumor response to anti-HGF therapy. The variable effects of L2G7 + cyclopamine and L2G7 + 5E1 combination therapies on survival reflect weakened inhibition of the targeted signaling pathways, especially HGF signaling. The mechanism of this effect remains unclear at this time. Considering the specificity of mAbs, we consider it highly unlikely that 5E1 interferes directly with the neutralization of HGF by L2G7. One possibility warranting further investigation is that combination therapy activates molecular feedback mechanisms that support c-Met receptor activation or stability. It is possible that therapeutic efficacy might be enhanced by direct pharmacologic inhibition of c-Met tyrosine kinase activity or targeting molecules downstream of c-Met in the phosphatidylinositol 3-kinase pathway. Alternatively, combination therapies might have different off-target effects that we cannot detect by analyzing effector molecules of Shh and HGF. Nevertheless, these results underscore the importance of preclinical testing of molecular-targeted therapies in animal models of tumors in which the targeted pathways are known to be active.

Disclosure of Potential Conflicts of Interest

K.J. Kim is employed by and has ownership interest in Galaxy Biotech. K.J. Kim also received commercial research support from Takeda Pharmaceuticals. J. Laterra received a commercial research grant from Galaxy Biotech and has ownership interest in Galaxy Biotech. J. Laterra is a consultant/advisory board member for Genentech and Merck.

Acknowledgments

The authors thank Kristin Kraus (University of Utah) for editorial assistance and Robert Lipinski (University of Wisconsin-Madison) for advice on cyclopamine pharmacology.

Grant Support

NIH CA108622 (D.W. Fults), NS43987 (J. Laterra), and CA129192 (J. Laterra).

The costs of publication of this article were defrayed in part by the payment of page charges. This article must therefore be hereby marked *advertisement* in accordance with 18 U.S.C. Section 1734 solely to indicate this fact.

Received 06/01/2010; accepted 06/28/2010; published OnlineFirst 08/31/2010.

References

1. Fomchenko EI, Holland EC. Mouse models of brain tumors and their applications in preclinical trials. Clin Cancer Res 2006;12:5288–97.
2. Crawford JR, MacDonald TJ, Packer RJ. Medulloblastoma in childhood: new biological advances. Lancet Neurol 2007;6:1073–85.
3. Gajjar A, Chintagumpala M, Ashley D, et al. Risk-adapted craniospinal radiotherapy followed by high-dose chemotherapy and stem-cell rescue in children with newly diagnosed medulloblastoma (St Jude Medulloblastoma-96): long-term results from a prospective, multicentre trial. Lancet Oncol 2006;7:813–20.
4. Packer RJ, Sutton LN, Atkins TE, et al. A prospective study of cognitive function in children receiving whole-brain radiotherapy and chemotherapy: 2-year results. J Neurosurg 1989;70:707–13.
5. Silber JH, Littman PS, Meadows AT. Stature loss following skeletal irradiation for childhood cancer. J Clin Oncol 1990;8:304–12.
6. Goodrich LV, Scott MP. Hedgehog and patched in neural development and disease. Neuron 1998;21:1243–57.
7. Weiner HL, Bakst R, Hurlbert MS, et al. Induction of medulloblastomas in mice by sonic hedgehog, independent of Gli1. Cancer Res 2002;62:6385–9.
8. Rao G, Pedone CA, Coffin CM, Holland EC, Fults DW. c-Myc enhances Sonic hedgehog-induced medulloblastoma formation from nestin-expressing neural progenitors in mice. Neoplasia 2003;5:198–204.
9. Hallahan AR, Pritchard JI, Hansen S, et al. The SmoA1 mouse model reveals that notch signaling is critical for the growth and survival of sonic hedgehog-induced medulloblastomas. Cancer Res 2004;64:7794–800.
10. Hatton BA, Villavicencio EH, Tsuchiya KD, et al. The Smo/Smo model: hedgehog-induced medulloblastoma with 90% incidence and leptomeningeal spread. Cancer Res 2008;68:1768–76.
11. Schüller U, Heine VM, Mao J, et al. Acquisition of granule neuron precursor identity is a critical determinant of progenitor cell competence to form Shh-induced medulloblastoma. Cancer Cell 2008;14:123–34.
12. Yang ZJ, Ellis T, Markant SL, et al. Medulloblastoma can be initiated by deletion of Patched in lineage-restricted progenitors or stem cells. Cancer Cell 2008;14:135–45.
13. Birchmeier C, Birchmeier W, Gherardi E, Vande Woude GF. Met, metastasis, motility and more. Nat Rev Mol Cell Biol 2003;4:915–25.

Published OnlineFirst August 31, 2010; DOI: 10.1158/1535-7163.MCT-10-0486

14. Abounader R, Laterra J. Scatter factor/hepatocyte growth factor in brain tumor growth and angiogenesis. Neuro-oncol 2005;7:436–51.
15. Bottaro DP, Rubin JS, Faletto DL, et al. Identification of the hepatocyte growth factor receptor as the c-met proto-oncogene product. Science 1991;251:802–4.
16. Eder JP, Vande Woude GF, Boerner SA, LoRusso PM. Novel therapeutic inhibitors of the c-Met signaling pathway in cancer. Clin Cancer Res 2009;15:2207–14.
17. Fan S, Meng Q, Laterra JJ, Rosen EM. Role of Src signal transduction pathways in scatter factor-mediated cellular protection. J Biol Chem 2009;284:7561–77.
18. Sharma SV, Bell DW, Settleman J, Haber DA. Epidermal growth factor receptor mutations in lung cancer. Nat Rev Cancer 2007;7:169–81.
19. Li Y, Lal B, Kwon S, et al. The scatter factor/hepatocyte growth factor: c-met pathway in human embryonal central nervous system tumor malignancy. Cancer Res 2005;65:9355–62.
20. Binning MJ, Niazi T, Pedone CA, et al. Hepatocyte growth factor and sonic hedgehog expression in cerebellar neural progenitor cells costimulate medulloblastoma initiation and growth. Cancer Res 2008;68:7838–45.
21. Romer JT, Kimura H, Magdaleno S, et al. Suppression of the Shh pathway using a small molecule inhibitor eliminates medulloblastoma in Ptc1(+/–) p53(–/–) mice. Cancer Cell 2004;6:229–40.
22. Sanchez P, Ruiz i Altaba A. *In vivo* inhibition of endogenous brain tumors through systemic interference of Hedgehog signaling in mice. Mech Dev 2005;122:223–30.
23. Goodrich LV, Milenkovic L, Huggins KM, Scott MP. Altered neural cell fates and medulloblastoma in mouse patched mutants. Science 1997;277:1109–13.
24. Wetmore C, Eberhart DE, Curran T. Loss of p53 but not ARF accelerates medulloblastoma in mice heterozygous for patched. Cancer Res 2001;61:513–6.
25. Holland EC, Hively WP, DePinho RA, Varmus HE. A constitutively active epidermal growth factor receptor cooperates with disruption of G1 cell-cycle arrest pathways to induce glioma-like lesions in mice. Genes Dev 1998;12:3675–85.
26. Federspiel MJ, Bates P, Young JAT, Varmus HE, Hughes SH. A system for tissue-specific gene targeting: transgenic mice susceptible to subgroup A avian leukosis virus-based retroviral vectors. Proc Natl Acad Sci U S A 1994;91:11241–5.
27. Ericson J, Morton S, Kawakami A, Roelink H, Jessell TM. Two critical periods of Sonic hedgehog signaling required for the specification of motor neuron identity. Cell 1996;87:661–73.
28. Kim KJ, Wang L, Su YC, et al. Systemic anti-hepatocyte growth factor monoclonal antibody therapy induces the regression of intracranial glioma xenografts. Clin Cancer Res 2006;12:1292–8.
29. Giangaspero F, Perilongo G, Fondelli MP, et al. Medulloblastoma with extensive nodularity: a variant with favorable prognosis. J Neurosurg 1999;91:971–7.
30. Chen JK, Taipale J, Cooper MK, Beachy PA. Inhibition of Hedgehog signaling by direct binding of cyclopamine to Smoothened. Genes Dev 2002;16:2743–8.
31. Lipinski RJ, Hutson PR, Hannam PW, et al. Dose- and route-dependent teratogenicity, toxicity, and pharmacokinetic profiles of the hedgehog signaling antagonist cyclopamine in the mouse. Toxicol Sci 2008;104:189–97.
32. Palma V, Ruiz i Altaba A. Hedgehog-GLI signaling regulates the behavior of cells with stem cell properties in the developing neocortex. Development 2004;131:337–45.
33. Wechsler-Reya RJ, Scott MP. Control of neuronal precursor proliferation in the cerebellum by sonic hedgehog. Neuron 1999;22:103–14.
34. Ruiz i Altaba A, Mas C, Stecca B. The Gli code: an information nexus regulating cell fate, stemness and cancer. Trends Cell Biol 2007;17:438–47.
35. Rudin CM, Hann CL, Laterra J, et al. Treatment of medulloblastoma with hedgehog pathway inhibitor GDC-0449. N Engl J Med 2009;361:1173–8.
36. Yauch RL, Dijkgraaf GJ, Alicke B, et al. Smoothened mutation confers resistance to a Hedgehog pathway inhibitor in medulloblastoma. Science 2009;326:572–4.
37. Toschi L, Janne PA. Single-agent and combination therapeutic strategies to inhibit hepatocyte growth factor/MET signaling in cancer. Clin Cancer Res 2008;14:5941–6.
38. Burgess T, Coxon A, Meyer S, et al. Fully human monoclonal antibodies to hepatocyte growth factor with therapeutic potential against hepatocyte growth factor/c-Met-dependent human tumors. Cancer Res 2006;66:1721–9.
39. Thompson MC, Fuller C, Hogg TL, et al. Genomics identifies medulloblastoma subgroups that are enriched for specific genetic alterations. J Clin Oncol 2006;24:1924–31.
40. Kool M, Koster J, Bunt J, et al. Integrated genomics identifies five medulloblastoma subtypes with distinct genetic profiles, pathway signatures and clinicopathological features. PLoS One 2008;3:e3088.
41. Northcott PA, Fernandez LA, Hagan JP, et al. The miR-17/92 polycistron is up-regulated in sonic hedgehog-driven medulloblastomas and induced by N-myc in sonic hedgehog-treated cerebellar neural precursors. Cancer Res 2009;69:3249–55.
42. Tabori U, Shlien A, Baskin B, et al. TP53 alterations determine clinical subgroups and survival of patients with choroid plexus tumors. J Clin Oncol 2010;28:1995–2001.
43. Tol J, Koopman M, Cats A, et al. Chemotherapy, bevacizumab, and cetuximab in metastatic colorectal cancer. N Engl J Med 2009;360:563–72.

Published OnlineFirst August 31, 2010; DOI: 10.1158/1535-7163.MCT-10-0486

Molecular Cancer Therapeutics

Molecular Therapy Targeting Sonic Hedgehog and Hepatocyte Growth Factor Signaling in a Mouse Model of Medulloblastoma

Valerie Coon, Tamara Laukert, Carolyn A. Pedone, et al.

Mol Cancer Ther 2010;9:2627-2636. Published OnlineFirst August 31, 2010.